Mon. Not. R. Astron. Soc. **311**, 869–876 (2000)

Calculations on the rates, mechanisms, and interstellar importance of the reactions between C and NH_2 and between N and CH_2

E. Herbst,[1]★ R. Terzieva[2] and D. Talbi[3]

[1]*Departments of Physics and Astronomy, The Ohio State University, Columbus, OH 43210, USA*
[2]*Department of Physics and Chemical Physics Program, The Ohio State University, Columbus, OH 43210, USA*
[3]*Laboratoire d'Etude Theorique des Milieux Extrêmes, Ecole Normale Supérieure, 24 rue L'Homond, F-75005 Paris, France*

Accepted 1999 September 15. Received 1999 August 9

ABSTRACT

The attempt to understand the temperature dependence of the HNC/HCN abundance ratio in interstellar clouds has been long standing and indecisive. In this paper we report quantum chemical and dynamical studies of two neutral–neutral reactions thought to be important in the formation of HNC and HCN, respectively – $C + NH_2 \rightarrow HNC + H$, and $N + CH_2 \rightarrow HCN + H$. We find that although these reactions do lead *initially* to the products suggested by astronomers, there is so much excess energy available in both reactions that the HCN and HNC products are able to undergo efficient isomerization reactions after production. The isomerization leads to near equal production rates of the two isomers, with HNC slightly favoured if there is sufficient rotational excitation. This result has been incorporated into our latest chemical model network of dense interstellar clouds.

Key words: molecular processes – ISM: abundances – ISM: clouds – ISM: molecules.

1 INTRODUCTION

Determining and explaining the abundance ratio of the well-known interstellar molecules HNC and HCN has occupied astrochemists for some time (Creswell et al. 1976; Snyder & Hollis 1976; Watson 1976; Herbst 1978; Goldsmith et al. 1981; Graedel, Langer & Frerking 1982; Schilke et al. 1992; Turner, Pirogov & Minh 1997; Hirota et al. 1998) and these species are in all well-known chemical model networks (e.g. Pineau des Forêts, Roueff & Flower 1990; Lee, Bettens & Herbst 1996; Millar, Farquhar & Willacy 1997). The metastable species HNC lies approximately 14.4 kcal mol^{-1} (1 kcal mol^{-1} = 503 K) above HCN in energy (Pau & Hehre 1982; Lee & Rendell 1991; Bowman et al. 1993), but the potential energy barrier separating the two species, 30.2 kcal mol^{-1} with respect to HNC, is large enough so that isomerization does not occur between thermalized species at low temperatures.

Early observations that the abundance ratio between HNC and HCN is on the order of unity in cold dense clouds led Watson (1976) to suggest that the dissociative recombination reaction,

$$HCNH^+ + e^- \rightarrow HNC + H, HCN + H, \quad (1)$$

produces the species HNC and HCN with near equal branching fractions, since the precursor ion is linear. This ion is produced in dense clouds by reactions such as that between the abundant ion C^+ and neutral ammonia (Marquette et al. 1985):

$$C^+ + NH_3 \rightarrow HCNH^+ + H. \quad (2)$$

Watson's suggestion was supported by an early phase-space calculation by Herbst (1978) and more recent quantum chemical calculations of the relevant potential surfaces by Talbi & Ellinger (1998) and Shiba et al. (1998). Detailed dynamical calculations, however, have not yet been undertaken on the calculated potential surfaces. For HNC and HCN to possess equal or near equal abundances, it is also necessary for the species to be depleted at about the same rate, which occurs if the depletion is via molecular ions since these two polar species have nearly the same dipole moment.

The increasing realization, however, that the HNC/HCN ratio exceeds unity in some cold clouds (see, e.g. Irvine & Schloerb 1984) led to the suggestion of additional routes to the formation of HNC. Brown (1977) suggested and Allen, Goddard & Schaefer (1980) calculated that the ion–molecule reaction between C^+ and NH_3 might produce a significant amount of the ion H_2NC^+ in addition to the linear ion $HCNH^+$; namely,

$$C^+ + NH_3 \rightarrow H_2NC^+ + H; \quad (3)$$

the metastable H_2NC^+ ion can then undergo a dissociative recombination reaction with electrons which, unless there is considerable rearrangement of the atoms, produces only HNC:

$$H_2NC^+ + e^- \rightarrow HNC + H. \quad (4)$$

A second suggestion involves the neutral–neutral reaction (Graedel et al. 1982)

$$C + NH_2 \rightarrow HNC + H. \quad (5)$$

★ E-mail: herbst@ohstpy.mps.ohio-state.edu

The particular products chosen are those which would occur in a direct chemical reaction, in which the C atom sticks to the nitrogen portion of the NH_2 and the H atom then exits. An analogous reaction possibly leading preferentially to HCN is

$$N + CH_2 \rightarrow HCN + H, \quad (6)$$

with a similar argument leading to the choice of products (Goldsmith et al. 1981). In some recent model calculations of cold clouds (Turner et al. 1997; Terzieva & Herbst 1998), this second reaction actually appears to dominate the formation of HCN at early times, while the first neutral–neutral reaction is of lesser importance. Most recently, Hirota et al. (1998) returned to the dissociative recombination of $HCNH^+$ and invoked the quantum chemical calculation of Shiba et al. (1998) to suggest that the dissociative recombination leads to HNC on 60 per cent of collisions and HCN on 40 per cent of collisions. In the absence of reactions (5) and (6), this ad hoc suggestion certainly leads to a higher abundance of HNC than of HCN. The hypothesis of Hirota et al. (1998) stems from their observations of the HNC/HCN abundance ratio in a variety of cold dark cloud cores in which, confirming and enlarging upon earlier work of Irvine & Schloerb (1984) and of Swade (1989), they found values from 0.54 to 4.5, with most cores possessing ratios exceeding unity.

To a trained physical chemist, the astronomical observations are puzzling because it is not facile for chemical reactions to produce metastable species in preference to their stable isomers. Unless the chemical reaction produces the metastable isomer with only a small amount of internal (rotational + vibrational) energy, the possibility of isomerization and equilibration after the chemical reaction looms and indeed must occur at a non-zero rate if the product vibrational energy exceeds the isomerization barrier (Brown, Burden & Cuno 1989). This is especially important in the interstellar medium, where relaxation of reaction products occurs only slowly by radiative emission so that isomerization can occur above the activation energy barrier much more efficiently than relaxation. As one aspect of our long-range programme in understanding the chemical reactions leading to the HNC/HCN balance in interstellar clouds, we (Talbi & Herbst 1998) investigated the reaction between C^+ and NH_3 and found that, although the metastable product H_2NC^+ is initially formed, the subsequent isomerization leaves $HCNH^+$ as the overwhelmingly dominant product, ruling out the H_2NC^+ hypothesis as an explanation for the HNC/HCN abundance ratio.

How much internal (especially vibrational) energy do the HNC and HCN products of the $HCNH^+$ dissociative recombination possess? While it is found (Butler, Babcock & Adams 1997; Tomashevsky, Herbst & Kraemer 1998) in the dissociative reaction between the ion HCO^+ and electrons that the CO fragment possesses little internal energy even when formed in its ground electronic state, analogous detailed studies of the $HCNH^+$ dissociative recombination have not yet been undertaken. Unless much of the large exothermicity of this reaction (as well as of reactions 5 and 6) does not go into vibrational energy of the HCN and HNC products, subsequent isomerization will readily occur, as has been studied quantum mechanically by Brown et al. (1989) and, more recently, by Lan & Bowman (1993) with widely differing results. Brown et al. (1989) find that the HNC/HCN ratio ends up typically as 1/20 for a system which starts with a large amount of internal energy and radiates it away while isomerizing, while Lan & Bowman (1993) show that, for specific wave packets, the HNC/HCN isomerization leads to an abundance ratio ≈ 0.2, which is still somewhat lower than a value obtained from a simple statistical calculation known as the 'RRKM' approach in the rotationless limit (Lan & Bowman 1993; Holbrook, Pilling & Robertson 1996).

Although the metastable molecule HNC has a puzzlingly high abundance in cold clouds, its abundance is significantly lower in warmer regions. In their compendium, Irvine, Goldsmith & Hjalmarson (1987) listed the abundance of HCN in the sources TMC-1, Sgr B2, and the Orion Ridge as a constant 2×10^{-8} with respect to H_2, while the abundance of HNC drops to 0.3×10^{-8} in Sgr B2 and to 0.04×10^{-8} in the Orion Ridge. The abundance of HNC is especially low in hot core regions (Irvine et al. 1987; Schilke et al. 1992; Ungerechts et al. 1997). Thus a complete understanding of the HNC/HCN abundance ratio requires, in addition to some explanation for the low temperature enhanced abundance of the metastable HNC, a further explanation for the disappearance of this species with increasing temperature. Astronomers have suggested that HNC, being the more conventionally reactive of the two isomers, possibly reacts with neutral atoms such as H and O with a small activation energy such that the reaction at 10 K does not occur, while the reaction at somewhat higher temperatures (50–100 K) does (e.g. Pineau des Forêts et al. 1990). Hirota et al. (1998) derive an activation energy for the HNC + H reaction of 190 K to fit the data with a steady-state chemical model. Our quantum chemical investigations indicate, however, that the activation energy for the H + HNC reaction is quite high ($\approx$2000 K), so that this reaction occurs efficiently only in regions higher than 300 K in temperature (Talbi, Ellinger & Herbst 1996). The reaction between HNC and O has not been studied in detail. Thus it can be said that our current understanding of the temperature dependence of the HNC/HCN abundance ratio is in as sorry a state as our understanding of the low temperature abundance ratio.

We report here new results, both quantum chemical and dynamical, on the products and rate coefficients of the neutral–neutral reactions between C and NH_2 and between N and CH_2. We find that the reactions do, at least initially, produce the products ascribed to them, however we also find that, if the reactions occur on their lowest energy potential surfaces, they are so exothermic that the HNC and HCN products have more than sufficient energy to isomerize in the interstellar medium. Isomerization competes with radiative relaxation, in the end producing nearly equal abundances of the two isomers, according to new statistical calculations reported here, which we feel are possibly more appropriate for the products of chemical reactions than the more detailed isomerization calculations reported heretofore. The statistical calculations are in reasonable (factor of 2) agreement with the wave packet calculations by Lan & Bowman (1993) in the rotationless limit, but the exact HNC/HCN abundance ratio depends on the rotational excitation of these species; a greater degree of rotational energy favours HNC, but only slightly. Our results have been put into a detailed model of dense cloud chemistry at 10 K.

2 QUANTUM CHEMICAL CALCULATIONS

The two reactions considered here are rather complex in that the open shell reactants lead to a variety of potential surfaces. For the ground-state reactants $N(^4S_u)$ and $CH_2(^3B_1)$, potential surfaces of spin multiplicity and symmetry $^{2,4,6}B_2$ arise, while for the ground-state reactants $C(^3P_g)$ and $NH_2(^2B_1)$, potential surfaces of spin multiplicity and symmetry $^{2,4}B_2$, $^{2,4}A_1$, and $^{2,4}A_2$ are formed. The symmetry designations refer to the C_{2v} point group. All of these

potential surfaces leading from reactants to products must be studied. They have been investigated at increasing levels of Møller–Plesset perturbation theory, namely MP2, MP3 and MP4, using GAUSSIAN 94 (Frisch et al. 1995). The characters of each stationary point (either minimum energy, for which all vibrational frequencies are real, or saddle point/transition state, characterized by one imaginary frequency) have been confirmed by vibrational analysis at the MP2/6-31G(d,p) level of theory.

For accurate electronic energies, single-point calculations have been performed at the MP4SDTQ/6-311++G(3df,3pd) level of theory with MP2/6-31G(d,p) optimized geometries. The calculations are at the full fourth-order level, and include contributions from single, double, triple and quadruple excitations while employing a triple-zeta basis set extended by polarization and diffuse functions. Such basis sets are known to give a large flexibility to the one-particle space, approaching the so-called Hartree–Fock limit. The electronic energies for the transition states and minimum energy states have been corrected for spin contamination from higher spin states, when needed, using an annihilation-projection method, the description of which can be found in Schlegel (1986). For comparison, stationary points have also been calculated with the CCSD(T) method using the same MP2/6-31G(d,p) optimized geometries and basis set. This is a coupled-cluster singles and doubles method (Raghavachari et al. 1989) with a perturbative treatment of the triple excitations. CCSD(T) numbers are not reported unless different from MP4 numbers. In such a case, they are given only for indication since there is no theoretical justification to choose one method over the other one.

In all cases, energies have been corrected for zero-point vibrational energy (ZPE); these corrections are made using carefully scaled vibrational wave numbers deduced from our previous theoretical study of the HCN and HNC systems (Talbi et al. 1996). The scaling factor is equal to 0.969 and has been applied to all molecules studied here.

The results for the potential surfaces of reactions (5) and (6) are shown in Figs 1 and 2, where the relative energies for reactants, products and intermediate stationary structures are listed in kcal mol^{-1}. Fig. 1 contains our results for the ground state potential surfaces for each reaction. For both reactions, the ground state potential surface is of $^2B_2$ symmetry and the reactants initially form a deeply-bound energy minimum ('complex') which then dissociates to products in their lowest electronic states – HNC($^1\Sigma$) + H for reaction (5) and HCN($^1\Sigma$) + H for reaction (6). In between the complexes and the products, there are saddle point ('transition state', or 'TS') structures but these are not of very high energy and do not inhibit reaction. As drawn in Fig. 1, the potential energy surfaces for reactions (5) and (6) appear rather distinct; whether they are distinct or not though depends on the potential barriers between them. We have calculated the path for isomerization between the complexes CNH_2 and NCH_2 and find it to be rather tortuous with the highest barrier being 36 kcal mol^{-1} with respect to the higher-lying complex.

Fig. 2 shows our results for the $C + NH_2$ and $N + CH_2$ reactions occurring on the excited but attractive quartet potential surfaces. (Other excited-state potential surfaces are repulsive, as shown in Fig. 2). The attractive excited state potential surfaces look very similar to the ground state surfaces but they are not as deep and they lead to the production of HNC and HCN in excited triplet states. The transition states in the exit channels lie at or near the energies of the reactants; i.e. at -0.1 kcal mol^{-1} for $(CNH–H)_{TS}$ and -1.1 kcal mol^{-1} for $(NCH–H)_{TS}$ so that reactions occurring on the potential surfaces (especially reaction 5) may occur slowly (see the discussion below). At the CCSD(T) level, we calculate these numbers to be respectively -2.7 kcal mol^{-1} and -5.1 kcal mol^{-1}, while values of -1.4 kcal mol^{-1} and -4.1 kcal mol^{-1} are given by Sumathi & Nguyen (1998). In Fig. 2, we indicate the uncertainties in the transition state energies by question marks.

Since the reactions that occur on the quartet potential surfaces are not very exothermic at all, the HNC and HCN products do not have much vibrational energy, at least while in their excited triplet states, rendering isomerization impossible. Subsequent radiative relaxation to their ground states can change this picture, however, depending on Franck–Condon factors.

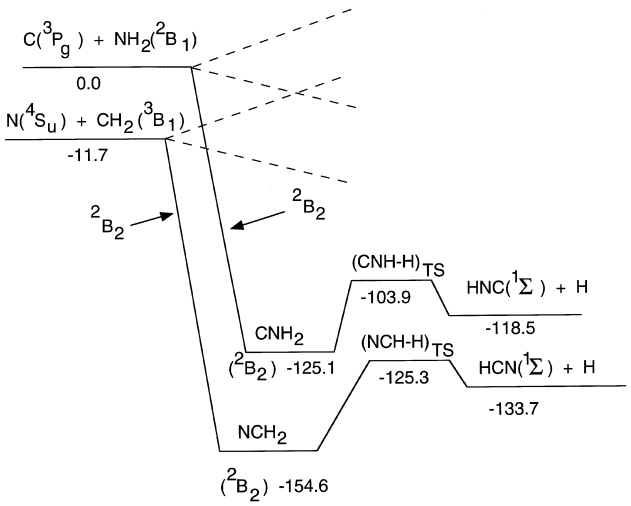

Figure 1. The ground-state potential surfaces for reaction of C with NH_2 and for N with CH_2 are shown. The calculated energies are in kcal mol^{-1} (1 kcal mol^{-1} = 503 K) and include zero-point energy effects as discussed in the text.

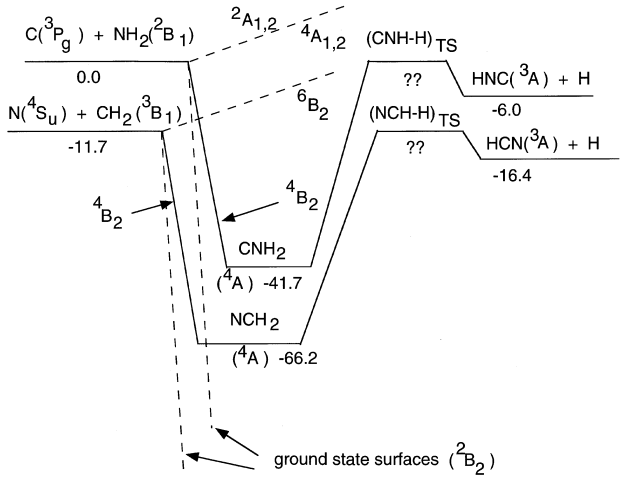

Figure 2. The excited-state but non-repulsive potential surfaces for reaction of C with NH_2 and for N with CH_2 are shown. The calculated energies are in kcal mol^{-1} (1 kcal mol^{-1} = 503 K) and include zero-point energy effects as discussed in the text. The exit channel transition states lie close to the energies of reactants.

3 RATE CALCULATIONS

Since the attractive potential energy surfaces for reactions (5) and (6) show no obvious entrance channel barriers, it is reasonable to use a long-range approximation to determine the rate coefficients, especially at low temperatures where this approximation is known to be most reasonable (Clary, Stoecklin & Wickham 1993; Woon & Herbst 1997). The long-range potential $V(R)$ for both reactions can be approximated as the dispersion potential (Hirschfelder, Curtiss & Bird 1954):

$$V(R) = -\frac{C_6}{R^6}, \tag{7}$$

if the somewhat smaller dipole–induced dipole term is neglected (Liao & Herbst 1995). The C_6 coefficient can be approximated by the formula

$$C_6 = \frac{3}{2}\frac{I_1 I_2}{I_1 + I_2}\alpha_1 \alpha_2, \tag{8}$$

where I_1 and I_2 are the ionization potentials of the reactants, while α_1 and α_2 are the isotropic dipole polarizabilities. The relevant polarizabilities have been calculated by us, while the ionization potentials are from standard sources. If every collision leads to a reaction, the rate coefficient $k(T)$ is given as a function of temperature by the formula (Liao & Herbst 1995)

$$k(T) = 2\left(\frac{2\pi}{\mu}\right)^{1/2}\Gamma\left(\frac{2}{3}\right)(2C_6)^{1/3}(k_B T)^{1/6}, \tag{9}$$

where μ is the reduced mass of reactants, Γ is the gamma function and k_B is the Boltzmann constant.

Since these are open shell systems with a variety of potential surfaces which correlate with reactants, it is necessary to consider which fraction of collisions lead to which potential surface. For the $C + NH_2$ system, we make an adiabatic approximation between the spin–orbit states of the neutral atomic carbon and the potential surfaces of CNH_2 formed from it. In particular, we assume that collisions with the lowest lying $^3P_0$ spin–orbit state correlate with the ground $^2B_2$ potential surface, while collisions with the first excited $^3P_1$ spin–orbit state correlate with the excited but attractive $^4B_2$ potential surface and with repulsive excited state surfaces. Collisions involving the highest spin–orbit state of C ($^3P_2$) all occur on excited repulsive surfaces. For the $N + CH_2$ system, there is no fine structure splitting and we assume that the potential energy surfaces for reaction are formed in proportion to their spin multiplicities.

3.1 C + NH_2

We assume that the spin–orbit states of C are thermalized, although for lower density clouds the state populations are probably subthermal. The fractional population of C atoms in their lowest spin–orbit state is then given by the inverse of the partition function $q(T)$:

$$q(T) = 1 + 3\exp(-23.6/T) + 5\exp(-62.6/T). \tag{10}$$

In addition to the reaction of carbon atoms in the lowest spin–orbit state via the attractive ground state potential surface, carbon atoms in the first excited spin–orbit state can react along the attractive quartet surface (Fig. 2), but the exit channel transition state energy lies very close to the energy of reactants. Any rotational energy in the system will add a centrifugal term to the transition state potential energy, so that any reaction will be hindered, especially at higher temperatures where the range of relative angular momenta is greater (Woon & Herbst 1997). In any case, reaction on the excited surface will probably not occur with an efficiency of anything near unity. We assume for simplicity that the reaction will occur only on the lowest energy surface. At low temperatures, any possible reaction on the excited state surface introduces no uncertainty into the adiabatic result since the population of the lowest C spin–orbit state dominates. Our results for the adiabatic rate coefficient as a function of temperature are listed in Table 1. Note that the rate coefficient is predicted to have an inverse relation on temperature. Thus, if this reaction were the dominant formation mechanism for HNC and it produced a stable version of this species, the inverse temperature dependence of the HNC abundance in dense clouds might be at least partially accounted for.

Table 1. Computed rate coefficients k for the reaction $C + NH_2 \rightarrow$ products along the ground state potential surface.

T (K)	k_{adiab} ($cm^3\,s^{-1}$)	k_{diab} ($cm^3\,s^{-1}$)
10	2.3×10^{-10}	3.3×10^{-11}
20	1.6×10^{-10}	3.7×10^{-11}
50	8.9×10^{-11}	4.3×10^{-11}
100	7.4×10^{-11}	4.8×10^{-11}
300	6.8×10^{-11}	5.8×10^{-11}

Had we ignored the C fine structure and made the (diabatic) assumption that the fraction of collisions occurring on each potential surface depends only on the statistical weight of the surface, we would have to multiply the result of equation (9) by the relative weight of the ground state surface, which is 1/9. This assumption, which leads to a significantly smaller rate coefficient at 10 K, is less likely, in our view, at cool interstellar temperatures given that the size of the C spin–orbit splitting is greater than the temperature. Nevertheless, the diabatic results are also listed in Table 1. At room temperature, the adiabatic and diabatic approximations yield pretty much the same result. If a significant percentage of the reaction occurs on the attractive excited state potential surface, the diabatic rate coefficients will all rise, while the adiabatic rate coefficients will rise only if the first excited spin–orbit state of C is populated.

3.2 N + CH_2

The ground state reactants can form potential surfaces of doublet, quartet and sextet spin multiplicity. Of these (see Figs 1 and 2) the sextet state is obviously repulsive. The quartet state is initially attractive but rises to a transition state only slightly below the energy of reactants. As with $C + NH_2$, any rotational energy in the system will add a centrifugal term to the transition state potential energy, so that the reaction will be hindered, especially at higher temperatures. Still, for this reaction, the computed range of transition state energies lies low enough that at low temperatures, reaction on the quartet surface may be significant. We ignore this possibility and make the simplifying approximation that reaction occurs predominantly on the ground potential energy surface. The probability that this surface is formed from reactants is 1/6, and this factor must be used with the result of equation (9). We calculate the rate coefficient ($cm^3\,s^{-1}$) to be $k_6(T) = 7.89\times10^{-11}(T/300)^{1/6}$. The result is expected to be most reliable at low temperatures. If reaction occurs with 100 per cent probability

along the excited quartet surface as well at low temperatures, the rate coefficient is three times as large since the statistical probability of forming either the ground or the first excited surface is 1/2. Since the long-range approximation used for our rate calculation tends to be high, we ignore the contribution of the excited state surface.

3.3 Energy of products

The exothermicity of reaction can go into the internal energy of the HNC or HCN product or into the relative translational energy between either molecule and H. A variety of experiments show that the most likely product translational energy is approximately equal to the energy difference between the exit channel transition state and the energy of products (Jarrold et al. 1986). For the $C + NH_2$ reaction occurring on the ground potential surface, the predicted most likely relative translational energy between HNC and H is $14.6\,\mathrm{kcal\,mol^{-1}}$, while the internal (vibrational–rotational) energy of HNC is $103.9\,\mathrm{kcal\,mol^{-1}}$. For the analogous $N + CH_2$ reaction, the predicted most likely relative translational energy between HCN and H is $8.4\,\mathrm{kcal\,mol^{-1}}$, while the internal energy of HCN is $113.6\,\mathrm{kcal\,mol^{-1}}$. Although these predictions are not definitive, they do strongly suggest that the product HNC and HCN molecules typically contain very large amounts of vibrational–rotational energy. If the rotational energy is sufficiently small, the vibrational energy will exceed that necessary for isomerization between HNC and HCN, and this process must be considered. The potential surface for isomerization in the absence of rotation is shown in Fig. 3. As the amount of internal rotational energy in the system increases, less is available for vibration. The rotational energy can be added to the potential energy to yield the effective potential energy. Since the rotational constants of HCN, HNC and the transition state between them are all different from one another, the effective energy surface rises unevenly as a function of rotational quantum number J. This is the only rotational quantum number considered since HCN and HNC are linear species and since we assume the transition state to be a spherical top. Once J becomes large enough such that the effective potential energy at the transition state is equal to the total internal energy of the product, then isomerization can no longer occur in the absence of tunnelling. Note that this limit will occur at a different value of J depending upon whether HNC is the initial product (reaction 5) or HCN is the initial product (reaction 6). For all higher J allowable by simple conservation of energy, there is no isomerization and the initial product of reaction (5) or (6) is stable.

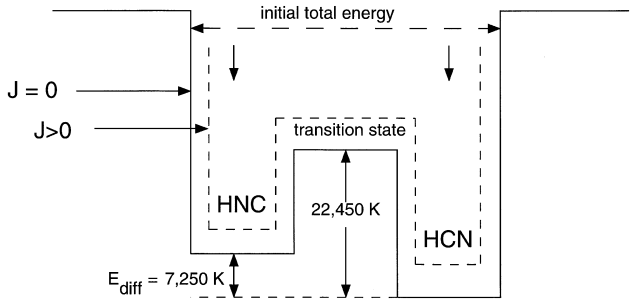

Figure 3. The effective potential energy surface for isomerization between the lower energy HCN and the higher energy HNC molecules, shown as a function of angular momentum J. Isomerization occurs in a statistical calculation until the system relaxes via the emission of radiation to an energy equal to the effective energy of the transition state. Tunnelling is excluded.

3.4 Isomerization?

According to simple RRKM statistical calculations (Holbrook et al. 1996), isomerization, if energetically allowed, is much more rapid than radiative relaxation unless the isomerizing species are quite large (DeFrees, McLean & Herbst 1985; Talbi & Herbst 1998). In particular, typical time-scales for the HNC/HCN system are $\approx 10^{-13}$ s for interconversion and $\approx 10^{-2}$ s for relaxation by one infrared photon (leading to an energy loss of ≈ 0.25 eV or $6\,\mathrm{kcal\,mol^{-1}}$). Thus, as relaxation slowly occurs, isomerization leads to equilibrated isomeric abundances at each internal energy. The final balance is determined at or near the effective barrier against isomerization, which is the energy of the transition state with rotational quantum number J. In the statistical (RRKM) limit, the final ratio of HNC to HCN product is given by the so-called equilibrium coefficient $K(E, J)$, which is defined according to the equation

$$K(E,J) = \frac{\rho^{\mathrm{HNC}}(E - E_{\mathrm{rot}}(J))}{\rho^{\mathrm{HCN}}(E + E_{\mathrm{diff}} - E_{\mathrm{rot}}(J))}, \tag{11}$$

where ρ stands for the density of vibrational states evaluated at either energy $E - E_{\mathrm{rot}}$ (HCN) or $E + E_{\mathrm{diff}} - E_{\mathrm{rot}}$ (HCN). The energy E is the total energy of HNC at the effective barrier against isomerization, $E + E_{\mathrm{diff}}$ is the total energy of HCN at the effective barrier against isomerization and E_{rot} is the rotational energy of either HNC or HCN.

Using the simple empirical function of Whitten & Rabinovitch (1964) for the vibrational density of states, we can obtain the equilibrium coefficient in the absence of any rotation to be equal to ≈ 0.84. As the rotational quantum number increases from zero, the equilibrium coefficient can change because the vibrational densities of states change unevenly. At $J = 83$ for reaction (6) and

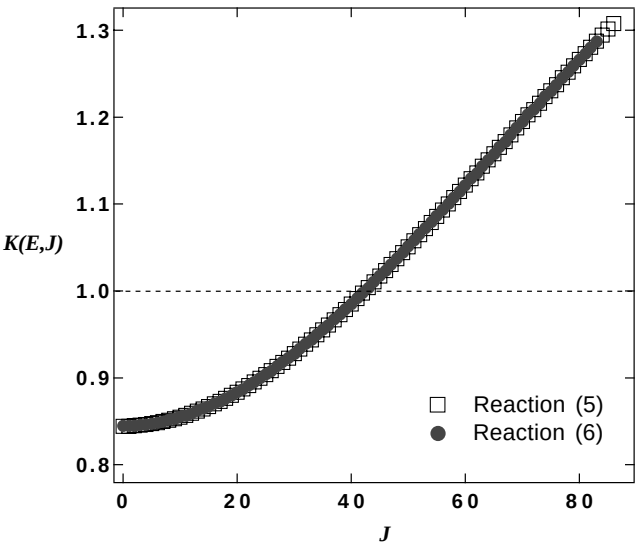

Figure 4. The equilibrium coefficient $K(E, J)$ for the HNC–HCN equilibrium is plotted versus rotational quantum number J. The energy E is the total energy of HNC at the effective barrier against isomerization – see text. The points for reaction (5) are identical with those for reaction (6) except for a few extra points at high J.

$J = 86$ for reaction (5), interconversion no longer becomes possible without tunnelling under the transition state barrier.

Plots of $K(E, J)$ versus J are shown for reaction (5) and (6) in Fig. 4. These differ only in the upper J limit at which isomerization ceases to occur. It can be seen that the equilibrium coefficient, although slightly below unity for $J = 0$, rises above unity by $J = 43$, and stays above unity until the maximum J at which isomerization is allowed. At still higher values of J, isomerization is possible only if tunnelling under the transition state barrier is as rapid as radiative relaxation. It is unlikely but not impossible that the amount of rotational energy in the products of either reaction would be sufficiently high to lead to such a high value of J for a significant fraction of products.

Although the use of the RRKM approach has been tested in many systems in chemistry (Holbrook et al. 1996), the isomerization between HNC and HCN is one of only a few systems which has been studied by more detailed quantum mechanical methods. Brown et al. (1989) calculated energies and wave functions of excited vibrational states of what they termed 'H + C + N', which is the entity existing above the transition state barrier in Fig. 3. Although their main concern was to study the 'H + C + N' produced by the dissociative recombination reaction between $HCNH^+$ and electrons, their analysis pertains to the products of reactions (5) and (6) as well. Brown et al. (1989) also followed the radiative relaxation, as it would occur in interstellar space, and concluded that HCN would be favoured over HNC by a factor of 20:1. They also concluded that their results are 'uncertain to about an order of magnitude' although they showed no detailed results in which HCN was favoured by a smaller amount than the 20:1 ratio. More recently, Bowman and collaborators (Bowman et al. 1993; Lan & Bowman 1993; Gazdy et al. 1995; Bowman, private communication) have looked with much more detail at the nature of the eigenstates and wave packets of 'H + C + N'. They find that some eigenstates are localized at the HCN position, some at the HNC position and some are delocalized between the two positions.

This theoretical work is supported by experimental work (e.g. Romanini & Lehmann 1993), which shows direct (weakly-allowed) vibrational transitions to states of HCN excited enough to be above the transition state to show narrow line widths, indicating a weak coupling to the HCN–HNC manifold. Although the delocalized states might be expected to relax radiatively to produce 50:50 mixtures of HCN and HNC, the fate of the localized states is less clear. For radiative relaxation to be more rapid than isomerization, the localized states would have to be stable for a period of $\approx 10^{-2}$ s, which is far too long for facile confirmation in the laboratory. More importantly, the results of chemical reactions are unlikely to be species in specific eigenstates but rather to be incoherent distributions over energy. These must be distinguished from wave packets, in which there is energy dispersion but with well-defined phases. The quantum mechanical study of Lan & Bowman (1993) uses wave packets to study the HNC–HCN isomerization in the absence of rotation and shows, for selected packets at higher vibrational energies than considered here, an HNC/HCN isomerization ratio of ≈0.20, which is lower than the statistical result. In our view, it is quite possible that the statistical result is the valid one for incoherent reaction products. It must be mentioned, however, that recent experiments by Amano, Nezu & Zelinger (1999) with a discharge in a gas mixture of CH_4 and N_2 lead to an HNC/HCN abundance ratio of 0.10 (Amano, private communication) which is much lower than our statistical analysis suggests. Of course, whatever reactions lead to HNC and HCN in the discharge, the products will not relax radiatively, as occurs in the interstellar medium. Rather, collisional relaxation is likely to occur and may be sufficiently rapid to compete with isomerization.

We conclude from these considerations the following points: (a) the nature of isomerization between metastable and stable structures such as HNC and HCN is still less than perfectly understood although statistical considerations, which work for many processes involving polyatomic molecules, indicate that for HNC/HCN a ratio near 1:1 and possibly somewhat greater can occur in the competition with radiative relaxation; (b) to avoid isomerization, the metastable species can be formed in a weakly exothermic reaction, or formed in a reaction that puts most of the energy into translation and/or rotation so that there is insufficient vibrational energy for subsequent interconversion. Based on studies of the reaction between HCO^+ and electrons, which show most of the non-electronic energy to go into translation between H and CO products (Tomashevsky et al. 1998; Butler et al. 1997), it is possible, although not proven, that the dissociative recombination reaction between $HCNH^+$ and electrons is similar. In particular, sufficient energy may go into translation to preserve the pristine branching fraction among the HCN + H and HNC + H product channels.

In the model results discussed below, we assume that the HCN, HNC products of reactions (5) and (6) undergo statistical interconversion but that the HCN, HNC products of the dissociative recombination reaction between $HCNH^+$ and electrons do not.

4 MODEL RESULTS AND DISCUSSION

Our current version of the gas-phase chemical network known as the 'new standard model' (Bettens, Lee & Herbst 1995) has been used. A fixed gas density n_H of 2×10^4 cm^{-3}, a cosmic-ray ionization rate ζ of 1.3×10^{-17} s^{-1} for H_2, and a temperature of 10 K, typical for dense cloud cores, have been chosen for the calculations. We have used a variety of gas-phase elemental abundances based on the so-called 'low metal' abundances (Lee et al. 1996; Terzieva & Herbst 1998) in which C/O = 0.42. Two types of depletions from the low-metal values – a relatively small depletion in the oxygen elemental abundance which raises the C/O ratio to 1.0, as well as a subsequent common depletion of a factor of 5 in the C and O elemental abundances – have been utilized.

Two different product branching fractions for the $HCNH^+ + e^-$ dissociative recombination reaction have been considered. In the '3:2 case', we use the assumption of Hirota et al. (1998) that the HNC + H channel has a branching fraction of 0.6, while HCN + H has a branching fraction of 0.4. Since recent storage ring experiments on other dissociative recombination products indicate that three-body channels can be important (Semaniak et al. 1998) we consider a second possibility labelled the '4.2:2.8:3 case', for which we assume that the HNC + H channel has a branching fraction of 0.42, the HCN + H channel has a branching fraction of 0.28 and a third channel – CN + H + H – has a branching fraction of 0.30. For this second case, the ratio of the HNC + H to the HCN + H product fraction is 1.5 as in the '3:2 case'.

The angular momentum range of the products for neutral–neutral reactions (5) and (6) (see Fig. 4) is such as to yield a range of HNC/HCN equilibrium coefficients $K(E, J)$ from 0.84–1.3 for both reactions. We have run models with three values for this coefficient – 0.84, 1.0 and 1.2. If we allow reactions (5) and (6) to occur on the bound excited state surfaces at low temperatures as

well, reaction (6) increases in rate more dramatically (with the adiabatic assumption for reactions 5) and produces additional HCN with too little energy to isomerize, unless the electronic energy can be efficiently converted into vibrational energy via non-diagonal Franck–Condon transitions. Thus, this assumption would tend to lower the calculated HNC/HCN formation ratio via reaction (6) to a value under that obtained from $K(E, J)$.

In all, twelve different models have been run; the parameters used in the various models are listed in Table 2. Table 3 contains calculated abundances of HCN and HNC with respect to the total hydrogen density, as well as the HNC/HCN abundance ratio for each model at both an early time (ET) of 1×10^5 yr and at steady state (SS). Note that the destruction rates for HNC and HCN are similar in our model at 10 K, so that variations in the HNC/HCN abundance ratio derive from formation pathways. Formation and destruction are not always easily delineated, however. If, for example, the formation rate of HNC gets quite large compared with HCN, the reaction between HNC and protons,

$$\mathrm{HNC} + \mathrm{H}^+ \rightarrow \mathrm{HCN} + \mathrm{H}^+, \quad (12)$$

can become an efficient formation mechanism for HCN, if not a major destruction mechanism for HNC.

A glance at the calculated HNC/HCN abundance ratios in Table 3 for each of the 12 models at both early time and at steady state shows that the ratios range from slightly below unity to almost 1.5, depending on what model parameters are utilized. The abundance ratios tend to be higher at steady state than at early time; the average of 12 models is 1.16 for early time and 1.31 for steady state. The observed average over the dense cores studied by Hirota et al. (1998) is ≈1.9 with a range larger than ours. A result of 1.5 indicates that the dissociative recombination between $HCNH^+$ and e^- is dominant in producing HCN and HNC while a lower result indicates the importance of neutral–neutral reactions. Thus, the dissociative recombination reaction appears to be more important at steady state than at early time. Given our choice for the $HCNH^+ + e^-$ branching fractions, there is no way that we can calculate a value for HNC/HCN greater than 1.5. It is clear that detailed dynamical studies of this crucial dissociative recombination have to be undertaken since our studies show that it remains the only mechanism which can possibly favour HNC over HCN to a significant extent.

Table 2. Model parameters.

Model	DR channels	$K(E, J)$	C/O	Depletion
1	3:2	0.84	0.42	1
2	3:2	1.0	0.42	1
3	3:2	1.2	0.42	1
4	3:2	1.0	0.42	5
5	3:2	1.0	1.0	1
6	3:2	1.0	1.0	5
7	4.2:2.8:3	0.84	0.42	1
8	4.2:2.8:3	1.0	0.42	1
9	4.2:2.8:3	1.2	0.42	1
10	4.2:2.8:3	1.0	0.42	5
11	4.2:2.8:3	1.0	1.0	1
12	4.2:2.8:3	1.0	1.0	5

Notes: two sets of product channels have been considered for the dissociative recombination (DR) reaction between $HCNH^+$ and electrons. See text.

For the neutral–neutral reactions, which form HNC and HCN, our detailed model results show that reaction (6) is far more important than reaction (5). This conclusion may be deceptive, however. Scott et al. (1998) have re-examined their earlier result on the reaction between N and H_3^+ and now find that no reaction occurs at a measurable rate. An update of our reaction network (Terzieva & Herbst 1998), in accordance with this result, leads to a relatively low abundance of ammonia and the related species NH_2, especially at early time. The underproduction of NH_2 in our models is most probably the reason for the contrast in the importance of reactions (5) and (6).

In addition to the neutral–neutral reactions studied here, the reaction of N atoms with methyl (CH_3) radicals is an important path for HCN formation. In our reaction network, we have incorporated the experimental studies of Marston, Nesbitt & Stief (1989), according to which the major products of this reaction (with a branching fraction of 0.9) are $H_2CN + H$ and a minor product channel leads to $HCN + H_2$. The H_2CN radical can in turn react with H atoms to produce HCN and H_2 according to Nesbitt, Marston & Stief (1990), although it is not clear that HNC is not formed as well. Even though the latter reaction is exothermic by ≈75 kcal mol^{-1}, we have assumed that further isomerization of the HCN is not likely to be efficient because, unlike the case for reactions (5) and (6), the available energy can be distributed among relative translational energy and the vibrational–rotational energy of both products, so that HCN might not possess internal energy large enough to overcome the isomerization barrier. Thus, the reaction of N atoms with methyl radicals is an 'independent' source of HCN which influences the HNC/HCN ratio.

The small calculated range of the HNC/HCN abundance ratio at 10 K is in contrast to the calculated abundances of the individual species, which vary over 1–2 orders of magnitude depending on

Table 3. Comparison of early-time (ET) and steady-state (SS) fractional abundances of HCN and HNC.

Model	HCN (ET)	HCN (SS)	HNC (ET)	HNC (SS)	HNC/HCN (ET)	HNC/HCN (SS)
1	5.8×10^{-8}	2.7×10^{-9}	6.5×10^{-8}	3.8×10^{-9}	1.11	1.43
2	5.8×10^{-8}	2.7×10^{-9}	6.6×10^{-8}	3.8×10^{-9}	1.15	1.43
3	5.7×10^{-8}	2.7×10^{-9}	6.7×10^{-8}	3.8×10^{-9}	1.18	1.44
4	2.6×10^{-7}	2.2×10^{-8}	3.6×10^{-7}	2.9×10^{-8}	1.38	1.34
5	3.4×10^{-7}	5.4×10^{-8}	4.4×10^{-7}	6.1×10^{-8}	1.28	1.14
6	6.9×10^{-7}	2.9×10^{-7}	9.8×10^{-7}	4.0×10^{-7}	1.43	1.37
7	3.9×10^{-8}	1.1×10^{-9}	3.6×10^{-8}	1.6×10^{-9}	0.93	1.38
8	3.8×10^{-8}	1.2×10^{-9}	3.7×10^{-8}	1.6×10^{-9}	0.97	1.37
9	3.7×10^{-8}	1.2×10^{-9}	3.8×10^{-8}	1.6×10^{-9}	1.02	1.37
10	9.7×10^{-8}	1.3×10^{-8}	1.1×10^{-7}	1.6×10^{-8}	1.15	1.26
11	2.0×10^{-7}	3.2×10^{-8}	2.1×10^{-7}	3.1×10^{-8}	1.08	0.98
12	3.3×10^{-7}	1.3×10^{-7}	4.1×10^{-7}	1.6×10^{-7}	1.26	1.20

Notes: the early-time abundances listed are for 1×10^5 yr.

time and model. The range of actual abundances for HCN is somewhat greater than that deduced by Hirota et al. (1998) from their observations, mainly because models with a high C/O abundance ratio and/or a depletion of five of these elements tend to overproduce HCN (as well as HNC) by an order of magnitude or more, especially at early times. Such models are best used under steady-state conditions. With this caveat, our models are in reasonable agreement with the observed range of HNC and HCN abundances.

Unlike the large differences in HNC and HCN abundances caused by elemental abundance variations, changes in the other parameters have far less effect. Comparison among Models 1–3, or among Models 7–9, for each of which $K(E,J)$ increases from 0.84 to 1.2, suggests that our results are almost entirely unaffected by the value of $K(E,J)$, at least in the range considered. Our assumptions concerning the products of $HCNH^+ + e^-$ affect the results to a greater extent. The abundances of HCN and HNC, produced in Models 1 through 6, for which the '3:2' dissociative recombination case is postulated, are all larger by factors of 2–3 than the analogous abundances produced by the corresponding Models 7 through 12. In addition, the HNC/HCN abundance ratio decreases with an increase in the branching fraction of the CN + H + H channel because smaller amounts of HNC and HCN are being made by the dissociative recombination route.

So far, we have only discussed model results at 10 K. The decrease in observed HNC abundance with increasing cloud temperature remains in need of an explanation since activation energy barriers greater than or equal to 3.3 kcal mol^{-1} ($\approx$1660 K) have been found for the previously favoured HNC + H reaction (Sumathi & Nguyen 1998; Talbi et al. 1996) so that it cannot deplete HNC rapidly at temperatures under 300 K. Studies of other likely neutral–neutral reactions, such as HNC + O or HNC + OH, may hold the key to a clarification of the temperature dependence of the HNC/HCN ratio.

ACKNOWLEDGMENTS

Parts of the calculations reported here were supported by the Institut du Développement et des Ressources en Informatique Scientifique (IDRIS); the support is gratefully acknowledged. EH acknowledges the support of the National Science Foundation for his research in astrochemistry. We wish to thank the Ohio Supercomputer Center for time on their T90 computer.

REFERENCES

Amano T., Nezu M., Zelinger Z., 1999, Proc. 54th Ohio State University Inter. Symp. Mol. Spectrosc., 54, 217
Allen T. L., Goddard J. D., Schfefer III H. F., 1980, J. Chem. Phys., 73, 3255
Bettens R. P. A., Lee H.-H., Herbst E., 1995, ApJ, 443, 664
Bowman J. M., Gazdy B., Bentley J. A., Lee T. J., Dalteo C. E., 1993, J. Chem. Phys., 99, 308
Brown R. D., 1977, Nat, 270, 39
Brown R. D., Burden F. R., Cuno A., 1989, ApJ, 347, 855
Butler J. N., Babcock L. M., Adams N. G., 1997, Mol. Phys., 91, 81
Clary D. C., Stoecklin T. S., Wickham A. G., 1993, J. Chem. Soc. Faraday Trans., 89, 2185
Creswell R. A., Winnewisser G., Pearson E. F., Winnewisser M., 1976, Sterne und Weltraum, 15, 118
DeFrees D. J., McLean A. D., Herbst E., 1985, ApJ, 293, 236
Frisch M. J. et al., 1995, Gaussian 94, Gaussian, Inc., Pittsburgh, PA
Gazdy B., Musaev D. G., Bowman J. M., Morukuma K., 1995, Chem. Phys. Lett., 237, 27
Goldsmith P. F., Langer W. D., Ellder J., Kollberg E., Irvine W., 1981, ApJ, 249, 524
Graedel T. E., Langer W. D., Frerking M. A., 1982, ApJS, 48, 321
Herbst E., 1978, ApJ, 222, 508
Hirota T., Yamamoto S., Mikami H., Ohishi M., 1998, ApJ, 503, 717
Hirschfelder J. O., Curtiss C. F., Bird R. B., 1954, Molecular Theory of Gases and Liquids. Wiley, New York
Holbrook K. A., Pilling M. J., Robertson S. H., 1996, Unimolecular Reactions. John Wiley & Sons Ltd., Chichester
Irvine W. M., Schloerb F. P., 1984, ApJ, 282, 516
Irvine W. M., Goldsmith P. F., Hjalmarson Å, 1987, in Hollenbach D. J., Thronson H. A., Jr, eds, Interstellar Processes. Reidel, Dordrecht, p. 561
Jarrold M. F., Kirchner N. J., Liu S., Bowers M. T., 1986, J. Phys. Chem., 90, 78
Lan B. L., Bowman J. M., 1993, J. Phys. Chem., 97, 12535
Lee T. J., Rendell A. P., 1991, Chem. Phys. Lett., 177, 491
Lee H.-H., Bettens R. P. A., Herbst E., 1996, A&AS, 119, 111
Liao Q., Herbst E., 1995, ApJ, 444, 694
Marquette J. B., Rowe B. R., Dupeyrat G., Poissant G., Rebrion C., 1985, Chem. Phys. Lett., 122, 431
Marston G., Nesbitt F. L., Stief L. J., 1989, J. Chem. Phys.,91, 3483
Millar T. J., Farquhar P. R. A., Willacy K., 1997, A&AS, 121, 139
Nesbitt F. L., Marston G., Stief L. J., 1990, J. Phys. Chem., 94, 4946
Pau G.-F., Hehre W. J., 1982, J. Chem. Phys., 86, 321
Pineau des Forêts G., Roueff E., Flower D. R., 1990, MNRAS, 244, 668
Raghavachari K., Trucks G. W., Pople J. A., Head-Gordon M., 1989, Chem. Phys. Lett., 157, 479
Romanini D., Lehmann K. K., 1993, J. Chem. Phys., 99, 6287
Schilke P., Walmsley C. M., Pineau des Forêts G., Roueff E., Flower D. R., Guilloteau S., 1992, A&A, 256, 595
Schlegel H. B., 1986, J. Chem. Phys., 84, 4530
Scott G. B. I., Fairley D. A., Freeman C. G., McEwan M. J., 1998, J. Chem. Phys., 109, 9010
Semaniak J. et al., 1998, ApJ, 498, 886
Shiba Y., Hirano T., Nagashima U., Ishii K., 1998, J. Chem. Phys., 108, 698
Snyder L. E., Hollis J. M., 1976, ApJ, 204, L139
Sumathi R., Nguyen M. T., 1998, J. Phys. Chem. A, 102, 8013
Swade D. A., 1989, ApJS, 71, 219
Talbi D., Ellinger Y., 1998, Chem. Phys. Lett., 288, 155
Talbi D., Herbst E., 1998, A&A, 333, 1007
Talbi D., Ellinger Y., Herbst E., 1996, A&A, 314, 688
Terzieva R., Herbst E., 1998, ApJ, 501, 207
Tomashevsky M., Herbst E., Kraemer W. P., 1998, ApJ, 498, 728
Turner B. E., Pirogov L., Minh Y. C., 1997, ApJ, 483, 235
Ungerechts H., Bergin E. A., Goldsmith P. F., Irvine W. M., Schloerb F. P., Snell R. L., 1997, ApJ, 482, 245
Watson W. D., 1976, Rev. Mod. Phys,., 48, 513
Whitten G. Z., Rabinovitch B. S., 1964, J. Chem. Phys., 41, 1883
Woon D. E., Herbst E., 1997, ApJ, 477, 204

This paper has been typeset from a TEX/LATEX file prepared by the author.